Journal of Applied Sciences

ISSN 1812-5654

science alert

ANSInet
an open access publisher
http://ansinet.com

Journal of Applied Sciences 9 (6): 1153-1158, 2009
ISSN 1812-5654

Prediction of Vertical Peak Ground Acceleration and Vertical Acceleration Response Spectra from Shallow Crustal Earthquakes

H. Aghabarati and M. Tehranizadeh
Department of Civil and Environmental Engineering, Amirkabir University of Technology, Tehran, Iran

Abstract: In this study, empirical ground-motion models for the vertical component from shallow crustal earthquakes are derived using worldwide strong ground-motions. Models are applicable to moderate and large magnitudes, distances 0-100 km and spectral periods of 0-10 sec. These attenuation relationships are presented for vertical peak ground acceleration and vertical acceleration response spectra in active tectonics regions. The effects of magnitude, distance, local average shear wave velocity, mechanism and nonlinear site response are included in these equations. The hanging wall effect is included with an improved model that varies smoothly as a function of the source properties and the site location. The standard deviation is magnitude dependent with smaller magnitudes leading to larger standard deviations.

Key words: Attenuation relationship, shallow crustal earthquake, faulting mechanism, hanging wall, nonlinear soil response

INTRODUCTION

Current studies of earthquake effects have tended to disregard the vertical ground motion and concentrate mainly on the horizontal component. The primary reason for this practice lies in the consideration that engineering structures have adequate resistance to dynamic forces induced by the vertical ground motion, which is generally much smaller than its horizontal components. If the effect of vertical motion is explicitly included in design, it is typically assumed that the ratio of vertical to horizontal (V/H) response spectra will not exceed two-thirds (UBC, 1997; GB50011-2001, EUROCODE-8).

However, observations in recent earthquakes, such as the 1994 Northridge, California, 1989 Loma Prieta, California, 1999 Chi-Chi, Taiwan and the 1995 Kobe, Japan have indicated that the rule-of-thumb ratio of two-thirds may not be a good descriptor of vertical ground motion (Yang and Sato, 2000; Bozorgnia and Campbell, 2004; Elgamal and He, 2004). For example, the three-dimensional records obtained at a borehole array site in Kobe, Japan during the 1995 Kobe earthquake deserve particular attention, which showed that the peak vertical acceleration at the surface was twice as high as the peak horizontal acceleration. An integrated analysis of this case history has suggested the key role of local site effects on the ground motion records (Yang and Sato, 2000; Yang *et al*., 2000).

On the other hand, large vertical component of near-fault earthquake records has been considered and damage potentials of vertical ground motion on engineering structures have been emphasized in recent years (Papazoglou and Elnashai, 1996; Diotallevi and Landi, 2000; Button *et al*., 2002).

In view of the fact that the effects of vertical ground motion are not well understood, special attention of this study is hence placed on the behavior of the vertical ground motion recorded during these recent large earthquakes. In this study, it is presented equations for estimating peak vertical acceleration and vertical absolute acceleration response spectra in terms of magnitude, source-distance, site conditions and other parameters for shallow earthquakes in the seismically active parts of the World. Comparisons are also made between these empirical equations and equations used widely in seismological researches. Some of the earlier conclusions are important for the development of design codes, which does not consider vertical earthquake spectra or limits for the near-field ratio of vertical to horizontal acceleration for damaging earthquakes.

MATERIALS AND METHODS

For these models, it is selected 751 free-field strong-motion records from 57 earthquakes following the free-field definition of Joyner and Boore (1981) using the criteria; $M_w \geq 5.2$, $R_{rup} \leq 100$(km) and $h \leq 20$(km). Table 1

Corresponding Author: H. Aghabarati, Department of Civil and Environmental Engineering, Amirkabir University of Technology, Tehran, Iran

Table 1: Summary of distribution of data in the set of records used with respect to geographical location and faulting mechanism

Category	No. of records	Percentage
Geographical location		
Western North America	631	84.02
Europe and Middle East	91	12.12
Other regions	29	3.86
Earthquake mechanism		
Reverse (Thrust)	512	68.18
Strike-slip	191	25.43
Normal	48	6.39

shown summary of distribution of data in the set of records used with respect to geographical location and faulting mechanism.

The records are uniformly distributed with respect to magnitude and distance and consequently the equations obtained based on this set of data are well constrained and representative of the entire data space: $0 \le R_{rup} \le 100$ (km) and $M_W \ge 5.2$. The strong motion parameters include corrected vertical peak ground acceleration (PGA) and 5% damped pseudo response spectral acceleration (PSA) at natural periods range from 0.01 to 10.0 sec. Definition of the size of an earthquake is in terms of M_W (Kanamori, 1997). The source-to-site distance is defined as the shortest distance between the recording site and the rupture plane of earthquakes. The faulting mechanism of an earthquake is classified based on rake angle into strike-slip, normal and reverse groups.

DEVELOPMENT OF ATTENUATION RELATIONS

A number of different regression methods exist for deriving attenuation relations, which affect in different ways the predictive equations. For this regression analysis, it is used random effects model. In this method the error is assumed to consist of two parts: an earthquake-to-earthquake component η, which is the same for all records from the same earthquake and a record-to-record component ε, which expresses the variability between each record not expressed by the earthquake-to-earthquake component (Abrahamson and Youngs, 1992; Joyner and Boore, 1993). The standard deviation of these two errors is found along with the coefficients. This method is thought to take better account of the fact that each record from the same earthquake is not strictly independent. This algorithm uses an iterative approach to find the maximum likelihood solution. There are two terms defining the standard deviation for the model: an inter-event term τ which is the standard deviation of the η and an intra-event term σ which is the standard deviation of the ε.

GROUND MOTION ATTENUATION MODELS

The median estimate of ground motion for the vertical component of PGA and PSA is given by:

$$\ln y = c_1 + f_1(M_W) + f_2(M_W) f_3(R) + f_4(F) + f_5(HW, R_{JB}, M_W, Dip) + f_6(V_{S30}, V_{lin}, PGA_{non-lin}, PGA_{rock}) \quad (1)$$

Scaling of magnitude: The magnitude scaling characteristics $f_1(M_w)$ and $f_2(M_w)$ are given by follow:

$$f_1(M_W) = c_3(M_W - 6.5) + c_8(T)(8.5 - M_W)^2, f_2(M_W) = c_2(T) + c_4(M_W - 6.5) \quad \text{for } M_W \le 6.5$$
$$f_1(M_W) = c_5(M_W - 6.5) + c_8(T)(8.5 - M_W)^2, f_2(M_W) = c_2(T) + c_6(M_W - 6.5) \quad \text{for } M_W > 6.5 \quad (2)$$

Coefficients C_3, C_4, C_5 and C_6 are held to be fix during regression analysis and supposed to be 1.323, -0.423, -1.842, 0.724 for vertical PGA and PSA.

Scaling of distance: The distance scaling characteristics are given by:

$$f_3(R) = \ln \sqrt{R_{rup}^2 + c_7(T)^2} \quad (3)$$

where, R_{rup} is the shortest distance between the recording site and the rupture plane of earthquake and the coefficient $c_7(T)$ is constrained to varying with period.

Scaling of faulting mechanism: The period dependence for the style of faulting mechanism is given by:

$$f_4(F) = c_9(T)FR + c_{10}(T)FS + c_{11}(T)FN \quad (4)$$

Scaling of hanging wall: The HW model is developed to including three tapers on Joyner-Boore distance R_{JB}, magnitude and dip as follow:

$$f_5(HW, R_{JB}, M_W, DIP) = c_{12}(T) HW h_1(R_{JB}) h_2(M_W) h_3(Dip) \quad (5)$$

$$h_1(R_{JB}) = \begin{cases} 1 - R_{JB}/30 & 0 \le R_{JB} < 30 \\ 0 & 30 \le R_{JB} \end{cases} \quad (6)$$

$$h_2(M_W) = \begin{cases} 0 & M_W < 6.0 \\ 2(M_W - 6) & 6.0 \le M_W < 6.5 \\ 1 & 6.5 \le M_W \end{cases} \quad (7)$$

$$h_3(Dip) = \begin{cases} 1 - (Dip - 70)/20 & Dip \ge 70 \\ 1 & Dip < 70 \end{cases} \quad (8)$$

For the regression analysis, only a single HW parameter $c_{12}(T)$ is estimated. The factor HW is set to 1.0 for sites affected by hanging wall.

Scaling of site response: Based on the Youngs's approach (Youngs, 1993), the linear and non-linear soil response is modeled by:

Table 2: Coefficients and statistical parameters from the regression analysis of vertical PGA and PSA

T (sec)	C_1	C_2	C_7	C_8	C_9	C_{10}	C_{11}	C_{12}	C_{13}	C_{15}	C_{16}	V_{lin}
0	2.986	-1.576	9.051	-0.035	-0.233	-0.483	-0.716	0.684	-0.360	0.514	0.529	760
0.025	3.604	-1.642	9.017	-0.027	-0.340	-0.555	-0.879	0.684	-0.335	0.514	0.529	407
0.04	4.470	-1.759	9.270	-0.021	-0.447	-0.626	-1.041	0.684	-0.310	0.514	0.529	233
0.05	5.025	-1.841	10.212	-0.022	-0.518	-0.674	-1.041	0.684	-0.290	0.514	0.529	192
0.075	4.880	-1.792	10.464	-0.020	-0.308	-0.529	-0.950	0.684	-0.230	0.514	0.529	196
0.1	4.574	-1.757	10.464	-0.021	-0.266	-0.383	-0.799	0.684	-0.250	0.514	0.529	257
0.12	4.384	-1.659	10.464	-0.022	-0.266	-0.403	-0.677	0.684	-0.260	0.514	0.529	299
0.15	4.018	-1.556	10.464	-0.032	-0.266	-0.432	-0.616	0.684	-0.280	0.514	0.529	357
0.2	3.590	-1.497	10.464	-0.050	-0.266	-0.482	-0.616	0.683	-0.310	0.514	0.529	453
0.3	2.934	-1.381	10.464	-0.065	-0.266	-0.581	-0.486	0.408	-0.440	0.514	0.529	532
0.4	2.522	-1.308	9.623	-0.080	-0.266	-0.630	-0.356	0.408	-0.500	0.514	0.529	535
0.5	2.111	-1.247	8.826	-0.095	-0.266	-0.630	-0.226	0.408	-0.600	0.514	0.529	535
0.75	2.077	-1.168	8.091	-0.131	-0.266	-0.525	-0.170	0.408	-0.690	0.514	0.529	535
1.0	2.042	-1.221	7.738	-0.171	-0.266	-0.420	-0.170	0.408	-0.700	0.514	0.529	535
1.5	1.986	-1.279	8.216	-0.227	-0.380	-0.476	-0.170	0.408	-0.720	0.520	0.529	535
2.0	1.902	-1.380	8.216	-0.299	-0.552	-0.560	-0.374	0.408	-0.730	0.538	0.556	535
2.5	1.832	-1.380	8.216	-0.358	-0.694	-0.630	-0.558	0.408	-0.735	0.572	0.584	535
3.0	1.762	-1.380	8.216	-0.400	-0.837	-0.630	-0.743	0.408	-0.740	0.606	0.611	535
3.5	1.692	-1.380	8.216	-0.431	-0.980	-0.630	-0.927	0.408	-0.745	0.640	0.639	535
4.0	1.621	-1.380	8.216	-0.455	-0.980	-0.630	-0.927	0.483	-0.750	0.673	0.666	535
4.6	1.565	-1.380	8.216	-0.469	-0.980	-0.630	-0.927	0.538	-0.750	0.707	0.694	535
5.0	1.480	-1.380	8.216	-0.487	-0.980	-0.630	-0.927	0.626	-0.750	0.707	0.694	535
6.0	1.208	-1.380	8.216	-0.506	-0.980	-0.630	-0.927	0.626	-0.727	0.707	0.694	535
7.0	0.909	-1.380	8.216	-0.510	-0.980	-0.630	-0.927	0.626	-0.704	0.707	0.694	535
8.0	0.604	-1.380	8.216	-0.505	-0.980	-0.630	-0.927	0.626	-0.684	0.707	0.694	535
9.0	0.330	-1.380	8.216	-0.500	-0.980	-0.630	-0.927	0.626	-0.667	0.707	0.694	535
10.0	0.071	-1.380	8.216	-0.492	-0.980	-0.630	-0.927	0.626	-0.650	0.707	0.694	535

$$f_6\left(V_{S30}, V_{lin}, PGA_{non-lin}, PGA_{rock}\right) = s_1\left(V_{S30}, V_{lin}\right) + s_2\left(PGA_{non-lin}, PGA_{rock}\right) \quad (9)$$

The linear site amplification equation is given by:

$$s_1\left(V_{S30}, V_{lin}\right) = c_{13}(T)\ln\left(\frac{V_{S30}}{V_{lin}}\right) \quad (10)$$

The nonlinear term is given by:

$$s_2\left(PGA_{non-lin}, PGA_{rock}\right) = c_{14}(T)\ln\left(\frac{PGA_{non-lin}}{PGA_{rock}(=0.1g)}\right) \quad (11)$$

The coefficients, V_{lin}, $c_{13}(T)$ and $c_{14}(T)$ are depend on period and V_{S30}. These coefficients are prescribed based on the on the study of Choi and Stewart (2005). $PGA_{non-lin}$ is the predicted PGA in (g) for rock site, as given in Eq. 1.

Scaling of standard deviation: The total standard deviation is considered to this bellow form:

$$\sigma_{total}(M_W) = \begin{cases} c_{15}(T) + \left(c_{16}(T) - c_{15}(T)\right)M_W & 5.0 \le M_W < 7.0 \\ c_{16}(T) & M_W \ge 7.0 \end{cases} \quad (12)$$

Regression analysis: This model includes a large number of coefficients. To arrive at a smooth model, the coefficients were smoothed in a series of steps. The final smoothed coefficients for the median ground motion are shown in Table 2. It should be noted that the quality of selected data is not sufficient at long periods (T>3 sec) to provide reliable spectral (Ambraseys *et al.*, 2005; Akkar and Bommer, 2006).

RESULTS OF THE EMPIRICAL MODELS

The median response spectra for the current model are shown in Fig. 1 for reverse and strike-slip faulting. In general, the predicted response spectra increase with magnitude. In the magnitude condition, large amplitude in median periods is observed when magnitude is increases. The effects of style of faulting mechanism and local site condition are plotted in Fig. 2. Predicted response spectra plotted for reverse event shows higher amplitude in median and long periods compared to strike-slip and normal events. As it is shown in Fig. 2, the behavior of spectral acceleration is significantly different with respect to site conditions for reverse faulting. At short periods, the amplitudes of soil site is greater than rock site for PSA and indicates the soil site may increase the amplitude of strong ground-motions in short to median periods. The amplitudes for soft soil and soft rock are somewhat higher at short periods and the amplitudes for firm rock and hard rock are significantly lower at long periods for the specific values of magnitude (M_W = 7.0) and distance (R_{rup} = 10 km) used in the evaluation. The short-period amplitudes for soft clays are found to be much higher than the other site categories in short to median periods, consistent with reduced nonlinear site effects.

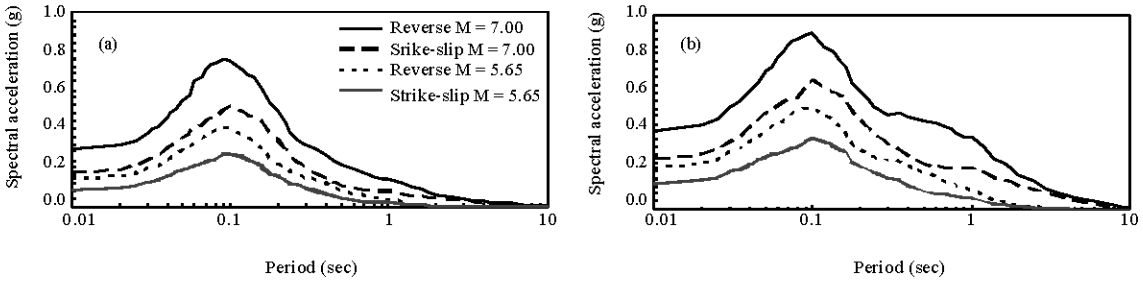

Fig. 1: PSA predicted from the ground-motion relations showing the effects of (a) magnitude for the rock site and (b) magnitude for the soil site

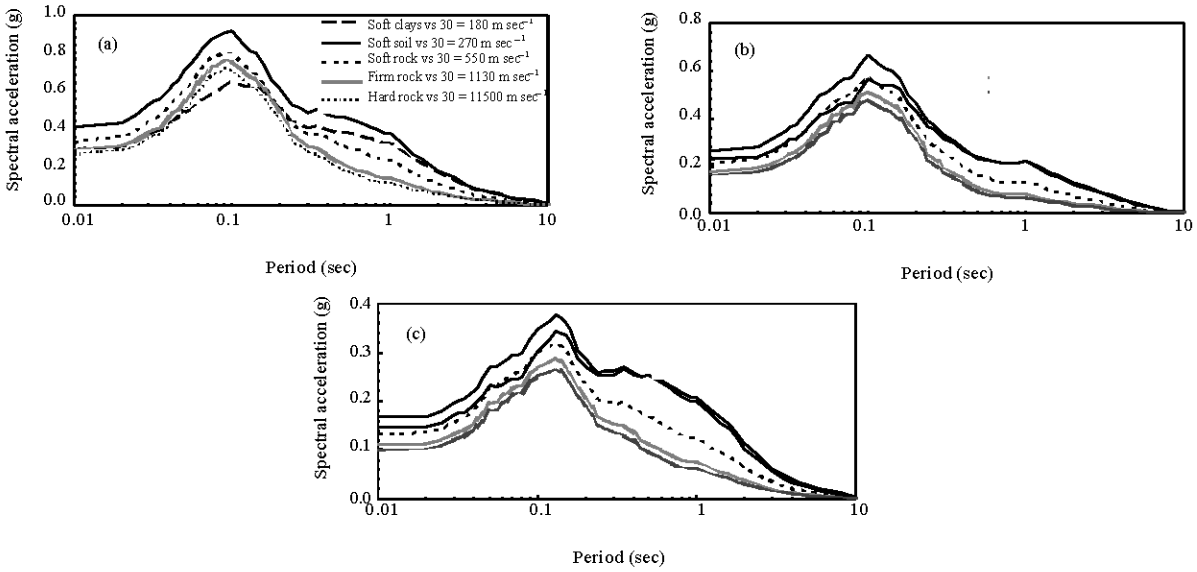

Fig. 2: PSA predicted from the ground-motion relations showing the effects of faulting mechanism (a) reverse, (b) strike-slip and (c) normal for different local soil conditions for the vertical component of ground-motion

Hard rock and firm rock have similar amplitudes at all periods. Figure 2 also shows the spectra tend to have higher amplitudes for reverse faulting at short to mid periods respected to other events.

The possibility of sites to be located over the hanging wall of reverse and thrust faults is higher than strike-slip and normal faults, which increases their ground-motion at close distances. The influence of local site condition is in general limited for strike-slip and normal faulting, although moderate effects are observed for soft rock at shorter periods and soft soil at longer periods.

DISCUSSION

These new ground-motion relations are compared to five ground-motion relations that are widely used to estimate horizontal response spectra for seismological and engineering analyses in non-extensional regions (Abrahamson and Silva, 1997; Campbell, 1997; Sadigh *et al*., 1997; Ambraseys and Douglas, 2003; Campbell and Bozorgnia, 2003). Almost all of the relations address the vertical component for both soil and rock.

They all define the faulting mechanism to strike-slip and reverse categories, where this study includes both reverse and strike-slip faulting as defined normal faulting. These relations use different definitions for local site conditions. Figures 3 and 4 show the predicted spectral acceleration from this ground-motion relation compared to predicted from five selected ground-motion relations for a site located 10 km from a reverse earthquake of $M_W = 7.0$. This distance corresponds to $R_{JB} = R_{rup} = 10$ km and Rseis = 10.4 km. The R_{seis} is defined as the shortest distance between the recording site and the zone of the

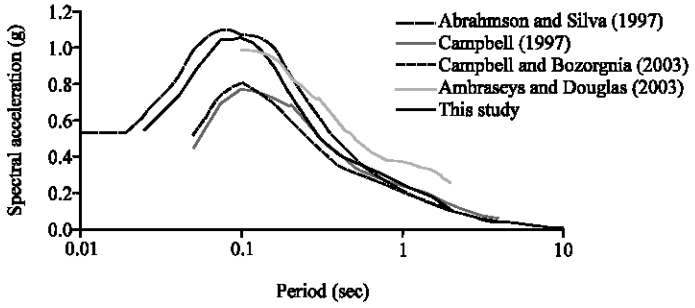

Fig. 3: Comparison of predicted PSA for generic soil from ground-motion relation in this study and five ground-motion relations widely used in seismology and engineering

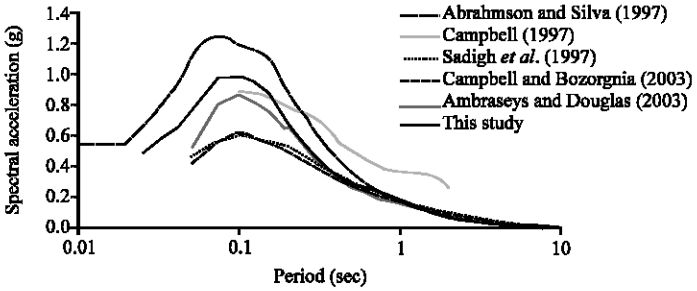

Fig. 4: Comparison of predicted PSA for generic rock from ground-motion relation in this study and five ground-motion relations widely used in seismology and engineering

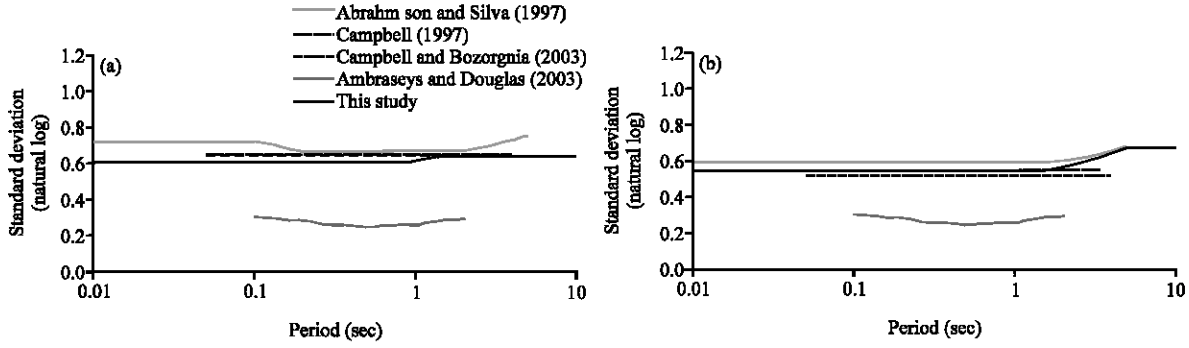

Fig. 5: Comparison of predicted standard deviations of spectral acceleration (σ_{lnY}) from this study and four ground-motion relations widely used in seismology and engineering (a) magnitude M = 5.5 and (b) magnitude M = 7.5

seismogenic energy release on the causative fault (Campbell, 1997). Comparisons are shown for the two most common site conditions used in engineering analysis, namely: generic soil, V_{S30} = 310 m sec^{-1} and generic rock, V_{S30} = 620 m sec^{-1} (Boore *et al*., 1997). In generally, the comparisons in Fig. 3 and 4 show that the relations predict spectral accelerations similar to those of the other five ground-motion relations when evaluated for generic soil and generic rock. This ground-motion relatively predicts higher amplitudes at short and median periods on generic soil. The prediction of these ground-motion relations relatively shows the same amplitudes at short periods for the vertical component on generic rock. Only this relation addressed these differences by site parameter, V_{S30} and the relation of Abrahamson and Silva (1997) and this relation incorporate nonlinear site effects. Figure 5 shows a comparison of the standard deviations (natural log) predicted from the ground-motion relations evaluated for two magnitudes. The standard deviation is important because it contributes significantly to deterministic and probabilistic estimates of ground-motion. Figure 5 indicates that the study vertical standard deviations are belonging to the lowest values.

CONCLUSIONS

The ground-motion relations developed in this study are considered valid to estimating vertical PGA and PSA for earthquakes from shallow crustal earthquakes. The study refines some new parameters in the model. Local site conditions do not significantly influence vertical spectra of strike-slip and normal faulting. However, we find that at long period vertical spectra for soft sites show systematically larger amplification than for stiff sites. This trend is reversed at short and intermediate periods. If this trend is genuine, it may suggest that decay of the high frequency motion in thin superficial soft soil deposits is due to high straining. The study shows that the median-predicted spectral accelerations among strike-slip, reverse and normal faulting earthquakes are different. These differences were found to become negligible at long periods, where dynamic stress drop is expected to have little effect on the amplitude of strong ground-motion. The standard deviation is magnitude dependent with smaller magnitudes leading to larger standard deviations.

ACKNOWLEDGMENT

This study was supported by the Institute of Earthquake Engineering and Seismology Research (IEESR) of Amirkabir University of Technology with grant No. 1-06-1384.

REFERENCES

Abrahamson, N.A. and R.R. Youngs, 1992. A stable algorithm for regression analyses using random effects model. Bull. Seismol. Soc. Am., 82: 505-510.

Abrahamson, N.A. and W.J. Silva, 1997. Empirical response spectral attenuation relations for shallow crustal Earthquakes. Seismol. Res. Lett., 68: 94-127.

Akkar, S. and J.J. Bommer, 2006. Influence of long-period filter cut-off on elastic spectra displacement. Earth. Eng. Struc. Dyn., 35: 1145-1165.

Ambraseys, N.N. and J. Douglas, 2003. Near-field horizontal and vertical earthquake ground motions. Soil Dyn. Earth. Eng., 23: 1-18.

Ambraseys, N.N., J. Douglas, S.K. Sarma and P.M. Smit, 2005. Equations for the estimation strong ground motions from shallow crustal earthquakes using data from Europe and the Middle East: Horizontal peak ground acceleration and spectra acceleration. Bull. Earth. Eng., 3: 1-53.

Boore, D.M., W.B. Joyner and T.E. Fumal, 1997. Equations for estimating horizontal response spectra and peak acceleration from western North American Earthquakes: A summary of recent work. Seismol. Res. Lett., 68: 128-153.

Bozorgnia, Y. and K.W. Campbell, 2004. The vertical-to-horizontal response spectral ratio and tentative procedures for developing simplified V/H and vertical design spectra. J. Earthq. Eng., 8: 175-207.

Button, M., C.J. Cronin and R.L. Mayes, 2002. Effect of vertical motions on seismic response of highway bridges. ASCE J. Struct. Eng., 128: 1551-1564.

Campbell, K.W., 1997. Empirical near-source attenuation relationships for horizontal and vertical components of peak ground acceleration, peak ground velocity, and pseudo-absolute acceleration response spectra. Seismol. Res. Lett., 68: 154-179.

Campbell, K.W. and Y. Bozorgnia, 2003. Updated near-source ground-motion (attenuation) relations for the horizontal and vertical components of peak ground acceleration and acceleration response spectra. Bull. Seismol. Soc. Am., 93: 314-331.

Choi, Y. and J.P. Stewart, 2005. Nonlinear site amplification as function of 30 m shear-wave velocity. Earth. Spect., 21: 1-30.

Elgamal, A. and L. He, 2004. Vertical earthquake ground motion record: An overview. J. Earthq. Eng., 8: 663-697.

Joyner, W.B. and D.M. Boore, 1981. Peak horizontal acceleration and velocity from strong-motion records including records from the 1979 Imperial Valley California Earthquake. Bull. Seismol. Soc. Am., 71: 2011-2038.

Joyner, W.B. and D.M. Boore, 1993. Methods for regression analysis of strong-ground data. Bull. Seismol. Soc. Am., 83: 469-487.

Kanamori, H., 1997. The energy release in grate Earthquake. J. Geophysic. Res., 82: 2981-2987.

Papazoglou, A.J. and A.S. Elnashai, 1996. Analytical and field evidence of the damaging effect of vertical Earthquake ground motion. J. Earthquake Eng. Struct. Dyn., 25: 1109-1137.

Sadigh, K., C.Y. Chang, J.A. Egan, F. Makdisi and R.R. Youngs, 1997. Attenuation relationships for shallow crustal Earthquakes based on California strong motion data. Seismol. Res. Lett., 68: 180-189.

Yang, J. and T. Sato, 2000. Interpretation of seismic vertical amplification observed at an array site. Bull. Seismol. Soc. Am., 90: 275-285.

Yang, J., T. Sato and X.S. Li, 2000. Nonlinear site effects on strong ground motion at a reclaimed island. Can. Geotech. J., 37: 26-39.

Youngs, R.R., 1993. Soil Amplification and Vertical to Horizontal Ratios for Analysis of Strong Motion Data from Active Tectonic Region, Appendix 2C in Guidelines for Determining Design Basis Ground Motions. Vol. 2, Appendices for Ground Motion Estimation, TR-102293 Electric Power Research Institute, Palo Alto, USA.